JOC The Journal of Organic Chemistry

Article

pubs.acs.org/joc

Pi-Extended Ethynyl 21,23-Dithiaporphyrins: A Synthesis and Comparative Study of Electrochemical, Optical, and Self-Assembling Properties

Ashley D. Bromby,[†] Samantha N. Keller,[†] Kevin J. A. Bozek,[‡] Vance E. Williams,[‡] and Todd C. Sutherland*[,†]

[†]University of Calgary, 2500 University Drive NW, Calgary, Alberta T2N 1N4, Canada

[‡]Simon Fraser University, 8888 University Drive, Burnaby, British Columbia V5A 1S6, Canada

Supporting Information

ABSTRACT: 21,23-Dithiaporphyrins were synthesized containing pi-extending ethynyl substituents at the meso positions. These porphyrins displayed highly bathochromic and broadened absorbance profiles spanning 400−900 nm with molar absorptivities ranging from 2500 to 300,000 M^{-1} cm^{-1}. Electrochemically, these ethynyl dithiaporphyrins undergo a single oxidation at 0.44 or 0.57 V and reduction at −1.17 or −1.08 V versus a ferrocene/ferrocenium internal standard depending on the type of functionalization appended to the ethynyl group. DFT calculations predict that the delocalization of the frontier molecular orbitals should expand onto the meso positions of the ethynyl 21,23-dithiaporphyrins; shrinking the HOMO−LUMO energy gap by destabilizing the HOMO energy. Indeed, the DFT results agree with our optical and electrochemical assessments. Finally, differential scanning calorimetry combined with cross-polarized optical microscopy and powder X-ray diffraction was used to assess the ability of these porphyrins for long-range order. For the ethynylphenyl alkoxy 21,23-dithiaporphyin, birefringent, soft-crystalline-like domains were observed by polarized microscopy, which are marginally sustained by a low-level of crystallinity detected in the XRD, suggesting that long-range ordering is possible. Overall, ethynyl 21,23-dithiaporphyrins are able to harvest much lower energy light and possess lower oxidation and reduction potentials compared to their pyrrolic analogues, which are desirable properties for applications in organic electronics.

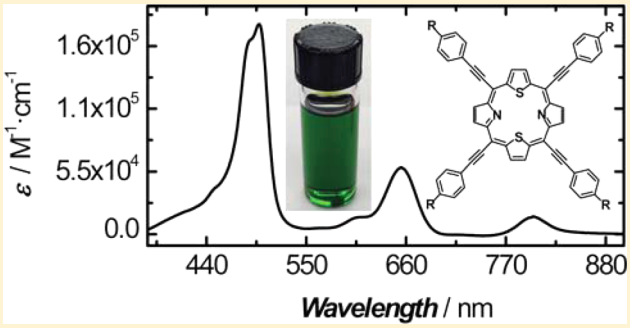

INTRODUCTION

Porphyrins are excellent light-harvesting compounds, which make them appealing candidates for applications such as photodynamic therapy[1−3] and dye-sensitized[4,5] and bulk-heterojunction solar cells.[6−8] The synthesis, optical, and electrochemical properties of porphyrins are well documented;[9−11] however, there remains motivation to improve the optical, electrochemical, and material properties of the porphyrin class. For applications in organic photovoltaics, improved properties include the following: bathochromically shifted absorbance profile to harvest low energy photons; lowered oxidation potentials to become stronger donor materials; and an attempt to impart long-range ordering on these materials through liquid crystalline phases. Core-modified 21,23-dithiaporphyrins, for example, have shown enhanced visible light absorption and facile redox properties compared to their nitrogen counterparts.[12−17] Recently, porphyrins have appeared in the materials community as highly efficient, even world-leading, components in photovoltaic power conversion efficiencies. Many of the highest performance compounds employ the "donor−acceptor" or "push−pull" approach to porphyrins, which are achieved through two sequential Sonogashira cross-coupling reactions of ethynyl moieties carried out after the porphyrin ring-closing step.[4,18−20] Under standard porphyrin synthesis conditions involving an aryl-aldehyde and pyrrole in the presence of a Lewis acid, the yields are usually low,[9] as such, there are practical motivations to avoid postporphyrin modifications. However, there are examples of optimized reaction conditions involving transition metal salts[21] or cocatalysts[22] that achieve between 55 and 65% yields. The most common synthetic approach[9] to obtain porphyrins, as well as 21,23-dithiaporphyrins, involves the use of *meso*-phenyl substituents; however, due to the out-of-plane phenyl spacer between the meso functional groups and the aromatic macrocycle, it is challenging to significantly tune the frontier molecular orbital (FMO) energies required for materials applications. The dihedral angles between the porphyrin aromatic ring and the *meso*-phenyl substituents typically ranges from 45° to 65°, as illustrated in Figure 1. Replacement of the phenyl spacer with an ethynyl linker to form 5,10,15,20-tetrakis(ethynylphenyl)-21,23-dithiaporphyrins

Received: June 9, 2015
Published: September 14, 2015

DOI: 10.1021/acs.joc.5b01299
J. Org. Chem. 2015, 80, 9401−9409

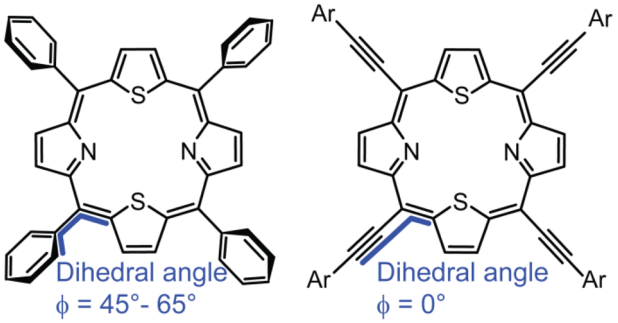

Figure 1. 5,10,15,20-tetrakisphenyl-21,23-dithiaporphyrin (left) and 5,10,15,20-tetrakis(ethynylphenyl)-21,23-dithiaporphyrin (right).

was sought to enable delocalization of the meso position functionality to the dithiaporphyrin core and affect FMO energies accordingly. Early reports of the addition of ethynyl spacers to the meso positions of porphyrins to enhance conjugation were reported by Arnold,[23] Anderson,[24] Lin,[25] and Boyle.[26] The synthesis of porphyrins bearing ethynyl meso substituents has been explored extensively for applications in solar cells,[27,28] sensors,[29] nonlinear optics,[30−32] and self-assembly.[33−35] To date, there are very few reports[24,36−41] of tetraethynylphenyl porphyrins and, to the best of our knowledge, no reports of tetraethynyl dithiaporphyrins. There are, however, examples of ethynyl porphyrins incorporating metals,[19,42] different aromatic groups in place of phenyl,[19,43] and polycyclic aromatic hydrocarbons fused to the backbones of the pyrrolic units.[44,45] Of the limited number of ethynylphenyl porphyrin syntheses reported, the optical properties were described;[18,19,21,23] however, electrochemical data is sparse. This work describes the synthesis of 5,10,15,20-tetrakis(ethynylphenyl)-21,23-dithiaporphyrins employing a novel synthetic method. Furthermore, the optical and electrochemical properties of these dithiaporphyrin derivatives were studied and, finally, the solid-state properties of these dithiaporphyrins were assessed.

RESULTS AND DISCUSSION

Synthesis. Typically, porphyrins with less than four *meso*-arylethynyl substituents are synthesized via reaction of TIPS-propynal and subsequent Sonogashira cross-couplings.[24,36−40] Dithiaporphyrin synthesis involves a synthetic route from 2,5-thiophene diols,[12−17,46] shown in Scheme 1, prior to the final macrocyclic ring-closing step. This diol formation synthetic step permits a cleaner macrocyclization reaction, resulting in easier purification because scrambling is largely suppressed. More importantly, the dithiaporphyrin synthetic approach is compatible with ethynyl precursors, which synthetically affords a 5,10,15,20-tetrakis(ethynylaryl) dithiaporphyrin product while avoiding postporphyrin modifications. Furthermore, the 2,5-thiophenediol precursor route could be exploited to form nonsymmetrical dithiaporphyrins[13−15] if desired.

The dithiaporphyrins in this work were synthesized to evaluate their potential as donor materials for organic electronic applications. As such, the following derivatives were synthesized: one with a weakly electron-donating alkyl group and one with a strong electron-donating ether group. Scheme S1 (see Supporting Information (SI)) shows the synthetic details, which afforded the ethynyl precursors **1a** and **1b** that were previously reported.[47,48] Briefly, the synthesis of the strong electron-donating substituent begins by alkylating 4-bromo-

Scheme 1. Synthesis of 5,10,15,20-Tetrakis(ethynylphenyl)-21,23-dithiaporphyrins[a]

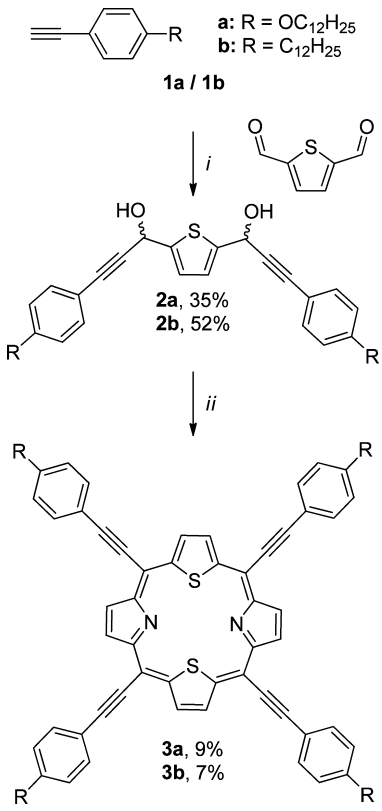

[a]Key: (i) (1) 2.2 equiv of *n*BuLi and TMEDA and (2) 1.0 equiv of 2,5-thiophenedicarboxaldehyde; (ii) (1) pyrrole and $BF_3{\cdot}OEt_2$ and (2) DDQ. See SI for synthesis of ethynyl precursors **1a**/**b**.

phenol as described in our previous synthetic work[16,17] to obtain 1-bromo-4-(dodecyloxy)benzene. The weakly electron-donating 1-bromo-4-dodecylbenzene was obtained by a Friedel−Crafts acylation[47] of bromobenzene with dodecanoyl chloride followed by a Wolff−Kishner reduction.[47] Both aryl bromides were then subjected to Sonogashira cross-coupling conditions with (trimethylsilyl)acetylene in modest isolated yields of 62 and 48% for 4-dodecyloxy[(trimethylsilyl)ethynyl]-benzene and 4-dodecyl[(trimethylsilyl)ethynyl]benzene, respectively. The two resulting silyl-protected alkynes were then deprotected using either tetrabutylammonium fluoride or K_2CO_3, which yielded comparable isolated yields of 45−55% for **1a** and **1b**. For the formation of the thiophene diols (Scheme 1), acetylides of **1a** and **1b** were formed by reaction with *n*BuLi in the presence of TMEDA, which were then added to half an equivalent of 2,5-thiophenedicarboxaldehyde (synthesized, but commercially available) to give 2,5-thiophenedicarbinols **2a** and **2b**. Diols **2a** and **2b** were isolated as a mixture of diastereomers and subjected to the final ring-closure by condensation with pyrrole in the presence of Lewis acid $BF_3{\cdot}OEt_2$ followed immediately by oxidation with DDQ to obtain dithiaporphyrins **3a** and **3b** with yields of 9 and 7%, respectively. Typical ring-closure and oxidation procedures for dithiaporphyrins[12−15,46] consist of two sequential 1 h steps. However, when the ethynyl dithiaporphyrins were subjected to these procedures, a mixture of unidentifiable products were observed. Lindsey and co-workers have extensively studied[49,50] the "optimal" ring-closing conditions for porphyrins and, therefore, a set of variable time reaction experiments were

DOI: 10.1021/acs.joc.5b01299
J. Org. Chem. 2015, 80, 9401−9409

conducted to find the optimal conditions for ethynyl dithiaporphyrins. Optimal conditions are defined as conditions that yield the desired product as well as unavoidable polymer as opposed to product, polymer, and unidentifiable, presumably not fully oxidized porphyrin-like species or scrambled species. It was found that for ethynyl dithiaporphyrins, room temperature conditions allowed the dithiaporphyrins to ring-close cleanly (as determined by TLC) only if both the ring-closing condensation followed by the DDQ oxidation step took place for no longer than 5 min each. The dramatic lowering of reaction time is presumably due to the highly delocalized, electron-rich intermediates formed.

Optical and Electrochemical Properties. Both dithiaporphyrins **3a** and **3b** display similar UV−vis absorption profiles and contain the Soret and Q-bands that are typical to porphyrins (Figure 2). Dithiaporphyrins **3a** and **3b** have

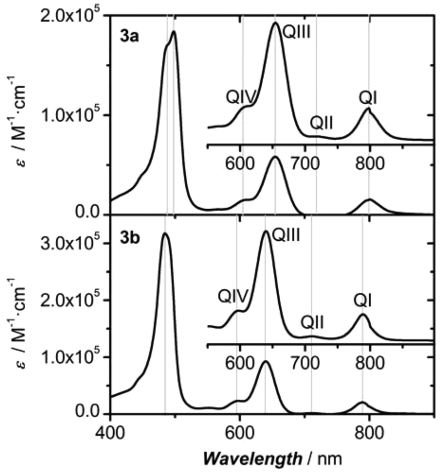

Figure 2. UV−vis absorption spectra of **3a** and **3b** (1×10^{-6} M) in methylene chloride. Insets: expanded Q-band region (1×10^{-5} M). The gray lines are peak positions of the Q-bands to allow visual comparison of the two derivatives.

dramatically red-shifted and broader absorption bands compared to the all-nitrogen analogues H_2TPP (5,10,15,20-tetrakisphenylporphyrin), H_2TEPP (5,10,15,20-tetrakis[4-ethylphenyl]porphyrin), H_2TEPOC_9 (5,10,15,20-tetrakis[4-nonoxyethynylphenyl]porphyrin), H_2TEPC_8 (5,10,15,20-tetrakis[4-octylethynylphenyl]porphyrin) as well as the *meso*-phenyl linked dithiaporphyrin $N_2S_2TPOC_{12}$ (5,10,15,20-tetrakis[4-dodecyloxyphenyl]-21,23-dithiaporphyrin) analogues outlined in Table 1. The incorporation of ethynyl spacers to the meso position has altered the absorption profile of these dithiaporphyrins such that they are green in solution (methylene chloride) and solid-state as opposed to the more typical purple for solid-state porphyrins and *meso*-phenyl dithiaporphyrins. The Soret band of dithiaporphyrins **3a** and **3b** exhibit bathochromic-shifts of approximately 40−50 nm and the onsets of absorption have been red-shifted a further 80−820 nm compared to 740 nm for our previous $N_2S_2TPOC_{12}$ dithiaporphyrins[16] and 670 nm for the H_2TPP porphyrins.[51] From the onset of absorbance, the estimated HOMO−LUMO energy gap of these ethynyl dithiaporphyrins **3a** and **3b** is ∼1.5 eV. Dithiaporphyrin **3a** has a slightly more red-shifted absorbance profile than **3b** due to the electron-donating phenyl ether groups. Furthermore, dithiaporphyrin **3a** exhibits splitting of the Soret band (Figure S1), indicating a break in degeneracy of the FMOs. The molar absorptivities for **3a** and **3b** (Table 1) are of the same order of magnitude as H_2TPP and $N_2S_2TPOC_{12}$ for the Soret bands as well as Q-bands I−IV, suggesting that none of the light-harvesting properties have been sacrificed to achieve a more broad band absorption profile. The oscillator strength of the Soret bands for **3a** and **3b** are 0.96 compared to 1.53 (greater than 1.0 due to the degeneracy for the Soret transition, which is typical for porphyrin Soret bands[52]) for $N_2S_2TPOC_{12}$. Despite the reduction in oscillator strength for the Soret bands for both ethynyl dithiaporphyrins, the transitions are broader when considering the full width at half-maximum (fwhm) values (Table S1) of 1753 and 1095 cm^{-1} for **3a** and **3b**, respectively, compared to $N_2S_2TPOC_{12}$ (776 cm^{-1}).

The major difference between the ethynyl dithiaporphyrins **3a** and **3b** absorption profiles compared to $N_2S_2TPOC_{12}$ is that Q-band III for **3a** and **3b** has a significantly higher molar absorptivity than Q-band IV, which is in contrast to $N_2S_2TPOC_{12}$ and H_2TPP where Q-band IV is usually the most intense, followed by Q-III, Q-I, and finally Q-II. Oscillator strengths for each Q-band transition for **3a** and **3b** as well as $N_2S_2TPOC_{12}$ were measured and summarized in Table S1. Oscillator strengths for the Q-bands of compound **3a** are as follows: 0.10, 0.20, 0.003, and 0.03, for Q-VI to Q-I, respectively. Note: dithiaporphyrin **3b** has very similar oscillator strengths to **3a**. Porphyrin $N_2S_2TPOC_{12}$ achieves similar oscillator strengths for Q-IV and Q-I (0.09 and 0.03, respectively); however, for Q-II, the oscillator strength is almost double (0.005) that of **3a**, and Q-III (0.08) is two and a half times less than **3a**. Clearly, the incorporation of the *meso*-ethynylphenyl substituents compared to the analogous *meso*-phenyl substitution results in dithiaporphyrins that are capable

Table 1. UV-Vis Absorption Properties for Compounds 3a and 3b[a]

	Soret	QIV	QIII	QII	QI	E_g^{opt} (eV)
H_2TPP[51,53]	417 (340)	515 (19)	548 (8)	592 (5.3)	648 (3.4)	1.9
H_2TEPP[37]	463		622		717	*b*
$N_2S_2TPOC_{12}$[16]	442 (300)	519 (25)	555 (14)	639 (1.9)	704 (7.3)	1.7
3a	489[c] (157)	612 (16)	655 (54)	719 (2.8)	797 (15)	1.5
	498[c] (182)					
H_2TEPOC_9[37]	472 (297)		600	653 (89.1)	744 (55.9)	*b*
3b	485 (311)	598 (17)	640 (61)	709 (2.7)	788 (15)	1.5
H_2TEPC_8[37]	466 (351)		599	642 (67.2)	737 (28.8)	*b*

[a]Absorption data are shown in nm followed by molar absorptivities in parentheses with units of 10^3 L mol^{-1} cm^{-1}. Absorption spectra of **3a** and **3b** were recorded in methylene chloride; $N_2S_2TPOC_{12}$ was recorded in toluene. E_g^{opt} was determined by the onset of absorbance; dithiaporphyrins **3a** and **3b** are not fluorescent. [b]Information not available. [c]Indicates maxima of both Soret bands.

DOI: 10.1021/acs.joc.5b01299
J. Org. Chem. 2015, 80, 9401−9409

Table 2. Electrochemical Properties for Compounds 3a and 3b[a]

	$E^{red2}_{1/2}$	$E^{red1}_{1/2}$	$E^{ox1}_{1/2}$	$E^{ox2}_{1/2}$	HOMO[e] (eV)	LUMO[e] (eV)	E_g^{EC} (eV)[f]
H_2TPP[57,58]	−1.95[b]	−1.63[b]	0.63[b]	0.90[b]	−5.43	−3.17	2.3
$N_2S_2TPOC_{12}$[16]			0.46[b]	0.68[b]	−5.26	−3.56[g]	1.7
3a		−1.17[c]	0.44[c,d]		−5.24	−3.63	1.6
3b		−1.08[c]	0.57[c,d]		−5.37	−3.72	1.6

[a]Electrochemical experiments were conducted in methylene chloride containing 0.1 M $(n\text{Bu})_4NPF_6$ with a polished platinum button working electrode, a Ag wire reference electrode, and a Pt wire counter electrode. All potentials are referenced to Fc/Fc^+. Half potentials are given in units of V. [b]Half potential obtained by cyclic voltammetry. [c]Half potential determined by differential pulse voltammetry at scan rate of 100 mV s^{-1}. [d]Irreversible oxidation. [e]Calculated based on Fc/Fc^+ E_{HOMO} = −4.8 eV.[59,60] [f]Calculated as the difference between the electrochemically estimated HOMO and LUMO energies. [g]Calculated by adding the onset absorbance energy (Table 1) to the electrochemically estimated HOMO energy.

of harvesting a wider range of lower energy photons over a larger amount of the visible spectrum.

Both dithiaporphyrins **3a** and **3b** display (Figure S2) an oxidation as well as a reduction (Table 2) when subjected to differential pulse voltammetry. Cyclic voltammetry was used to assess reversibility and, for both dithiaporphyrins **3a** and **3b**, electrochemical oxidation was found to be irreversible and the reduction quasi-reversible. The electrochemical properties of ethynyl dithiaporphyrins **3a** and **3b** are different compared to the $N_2S_2TPOC_{12}$ dithiaporphyrins, which exhibit two stepwise, one-electron reversible oxidations and no observable reduction reaction within the methylene chloride solvent window.[16] However, the oxidation potentials for **3a** and **3b** at 0.44 and 0.57 V, respectively, are comparable to the first oxidation potential for $N_2S_2TPOC_{12}$ at 0.46 V.[16] The oxidation peak potential is reflective of the HOMO energy level, and the results are as expected because the electron-rich alkoxy **3a** is easier to oxidize than its alkyl analogue **3b**. In a similar fashion, the reduction potential provides an estimate of the LUMO energy of a molecule. As such, the electron-donating effects, which destabilize the HOMO energy, also tend to destabilize the LUMO energy, rendering the molecule more difficult to reduce, which is mirrored by the lower reduction potential of **3b** (−1.08 V) compared to that of **3a** (−1.17 V). With estimates of the HOMO and LUMO energy values by electrochemical methods, it enables a crude estimate of the HOMO−LUMO energy gap at 1.6 eV for both **3a** and **3b**, which is comparable to the optical assessment, using the onsets of absorption, of the HOMO−LUMO energy gap at 1.5 eV. Dithiaporphyrins **3a** and **3b** oxidize at modest but similar potentials to $N_2S_2TPOC_{12}$ and significantly lower potentials than H_2TPP; however, these dithiaporphyrins are much easier to reduce than their H_2TPP counterparts by ∼0.5 eV, presumably due to highly delocalized and stabilized LUMOs. The electrochemical properties for both dithiaporphyrins show compatibility with the typical acceptor material [6,6]-phenyl C_{61} butyric acid methyl ester (PCBM) for photovoltaic applications. A standard poly(3-hexylthiophene-2,5-diyl) (P3HT) and PCBM photovoltaic cell have LUMO energies of −3.2 eV (relative to vacuum) for P3HT and −4.2 eV for PCBM.[54] Using 0.3 eV as the minimum energy difference[54−56] needed between the donor and the acceptor LUMOs to achieve a favorable driving force for electron transfer, the LUMO of an "idealized" donor is placed at −3.9 eV. Indeed, dithiaporphyrins **3a** and **3b** exhibit LUMO energies of −3.63 and −3.72 eV, respectively. Furthermore, the HOMO−LUMO energy gap of these dithiaporphyrins (1.6 eV) compares favorably to the band gap of P3HT (2.0 eV) and indicates an improved low-energy photon absorbing material.[54−56]

DFT Computations. DFT calculations at the B3LYP/6-31G+(d) level using Gaussian09[61] were performed on model dithiaporphyrins **3a** and **3b** to assess the extent of delocalization of the frontier molecular orbitals (FMO) from the macrocyclic core to the meso positions and roughly estimate the HOMO−LUMO energy gap. Optimized geometries were obtained by replacing alkyl fragments with methyl groups. In other nonethynyl porphyrin systems, the dihedral angle of the phenyl group to the macrocyclic core limits delocalization and therefore electronic tunability of the molecule. Indeed, DFT calculations indicate both the HOMO and LUMO (Figure 3 and Figure S3) have significant

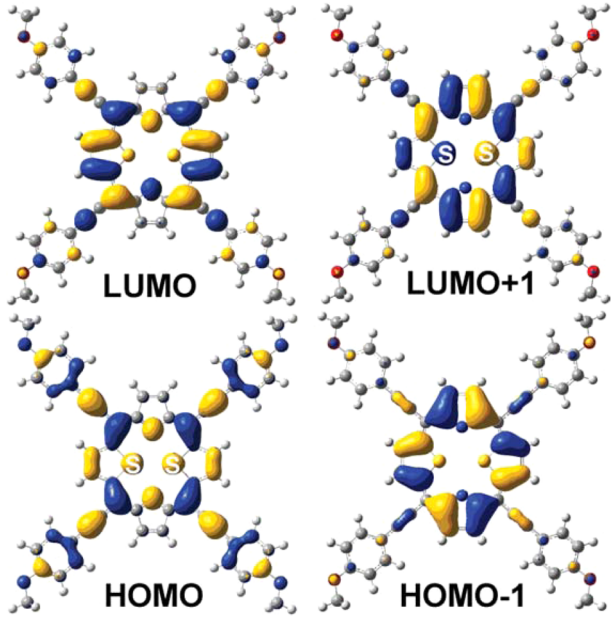

Figure 3. Frontier molecular orbitals of dithiaporphyrin **3a** using DFT methods at the B3LYP/6-31G(+)d level.

contributions from both the macrocyclic core and the *meso*-ethynylphenyl substituents. The DFT calculations estimate the HOMO−LUMO energy gap to be ∼2.0 eV, which is higher than both optically and electrochemically derived estimates of 1.5 and 1.6 eV for **3a** and **3b**, respectively. However, the approximation of HOMO−LUMO energies is sufficient at this level of DFT, accurately models the FMOs, and is commonly used for porphyrin systems.[62−65]

Solid-State Properties. Differential scanning calorimetry (DSC) thermograms of both dithiaporphyrins at 5 °C min^{-1} from −50 to 140 °C revealed that derivative **3b** was not liquid crystalline (LC) as the DSC trace (Figure S4) shows only recrystallization and melting transitions. However, the DSC

DOI: 10.1021/acs.joc.5b01299
J. Org. Chem. 2015, 80, 9401−9409

thermogram of **3a** (Figure 4) during heating showed several phase transitions, which were mirrored in the cooling trace.

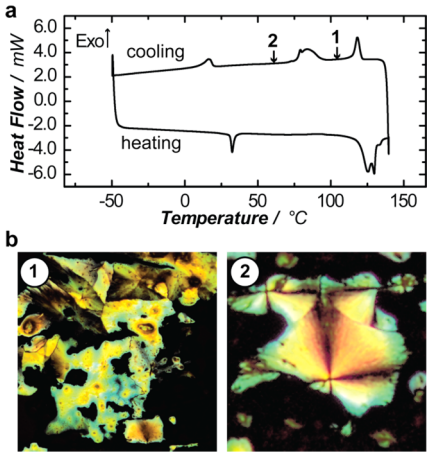

Figure 4. (a) DSC thermogram of dithiaporphyrin **3a** at 5 °C min^{-1} showing the 2nd heating and cooling cycles and points (1) and (2) refer to the temperatures where optical images were recorded. (b) Cross polarized optical microscopy images of dithiaporphyrin **3a** obtained during the cooling cycle at 200× magnification at 100 °C (1) and 60 °C (2).

Using peak deconvolution, enthalpies of each transition were determined, are summarized in Table 3, and are consistent with

Table 3. DSC Thermograms Detailing Transition Enthalpies and Temperatures for Compound 3a[a]

		heating cycle		cooling cycle[c]	
	transition[b]	T (°C)	ΔH (kJ/mol)	T (°C)	ΔH (kJ/mol)
3a	SC → SC	32.5	7.1	16.4	9.8
	SC → SC	125.4	48.1	79.0	1.7[d]
	SC → SC	129.6	7.7	84.0	29.5[d]
	SC → L_{ISO}	133.5	2.8	118.1	14.0

[a]DSC thermograms were obtained at rate of 5 °C min^{-1} for both the heating and cooling cycles. [b]Phase transitions were assigned using X-POM as well as powder XRD. [c]Phase transition assignments are in reverse order for the cooling cycle. [d]Because of hysteresis and transition kinetics, these phase transitions overlap.

other phase transition enthalpies for porphyrins reported in the literature.[66−68] On the basis of the thermogram of the heating cycle, dithiaporphyrin **3a** is likely either crystalline (Cr) or soft crystalline (SC) from −50 to 129.6 °C, whereby it undergoes a number of transitions between Cr or SC phases. Dithiaporphyrin **3a** clears to an isotropic liquid (L_{ISO}) at 133.5 °C.

Cross-polarized optical microscopy images for dithiaporphyrin **3a** were obtained upon cooling the compound from the isotropic liquid phase, as the hysteresis allowed for larger separation of phase transition peaks. As dithiaporphyrin **3a** cools from 118 to 96 °C, distinct birefringent domains appear (Figure 4b), and upon further cooling from 96 °C to room temperature, cross-type patterns begin to emerge (Figure 4b), which have been previously observed for hexagonally stacked discotic porphyrins.[68,69] However, these birefringent optical features are not necessarily conclusive for phase identification. Interestingly, when the domains shown in Figure 4b are sheared between two glass slides, the domains smear and lose their birefringence, indicating a mechano-responsive film that slowly regains its birefringence over the course of days. Collectively, the optical microscopy and DSC data suggest **3a** is either a soft crystal or liquid crystalline material. The large hysteresis (15 °C) of the isotropic transition temperature between the cooling and heating runs is consistent with a transition from a soft crystal rather than from a liquid crystal phase.

X-ray diffraction (XRD) at room temperature and elevated temperature (Figures S5 and S6) of porphyrin dithiaporphyrin **3a** affords only weak peaks over the range of angles observed, which might suggest low levels of crystallinity. However, becasuse of the large size of the porphyrin, which has a calculated diameter of ∼55 Å, we anticipate that the most intense diffraction peaks would appear at smaller angles than can be resolved with our instrumentation. As such, the crystalline and/or liquid crystalline ordering of this system cannot be unambiguously assigned within the limits of available instrumentation. Despite these challenges, the observation of birefringent domains by polarized microscopy clearly indicates some crystalline order, and it is postulated that dithiaporphyrin **3a** forms soft-crystalline material over a range of −50 to 130 °C.

■ CONCLUSIONS

In summary, two ethynyl 21,23-dithiaporphyrins were synthesized, which possess significant bathochromic-shifted absorbance profiles, high molar absorptivities, and broadened peaks compared to their pyrrolic analogues. Clearly, the ethynyl-linked meso positions enable significant electronic tuning that is absent in the tetrakis-phenyl variant porphyrins. Redox studies revealed that these dithiaporphyrins undergo a single oxidation and reduction at modest, albeit lower, potentials than comparable porphyrins. Finally, DSC, cross-polarized optical microscopy, and XRD results suggest there is potential, long-range order to these molecules, but a definitive structure remains elusive. The combination of both the optical and electrochemical assessment of these porphyrins shows that the inclusion of an ethynyl group to the meso position of 21,23-dithiaporphyrins results in the improvement of the ability of this class of compound to absorb photons and potentially act as a donor material for organic electronic applications.

■ EXPERIMENTAL SECTION

All chemicals were used as received without further purification unless otherwise specified. Column chromatography was performed on silica gel (230−400 mesh). Thin-layer chromatography was carried out on silica gel glass-backed TLC plates. Solvents were used as received or dried using a solvent purification system, and reactions were typically carried out under N_2 atmosphere. NMR spectra were recorded on a 300, 400, or 600 MHz spectrometer. Residual solvent peaks were as follows: chloroform, 7.26 ppm; ethyl acetate, 2.05, 4.12, and 1.26 ppm. Mass spectra were recorded with an ESI Q-TOF spectrometer or MALDI-TOF, and UV−vis spectra were recorded using a spectrophotometer in dual beam mode. Differential calorimetry thermograms were collected under N_2 atmosphere. Cross polarized optical microscopy was carried out on a microscope equipped with a heating stage.

Powder X-ray diffraction samples were heated to the isotropic liquid phase on a hot plate and loaded by capillary action. The excess material was cleaned off the sides with clean dry tweezers. Capillaries were then cut to length and mounted in a capillary furnace.[70] Measurements were carried out on a rapid diffractometer using Cu Kα radiation (λ = 1.5418 Å), a graphite monochromator, and a curved image plate (460 mm × 256 mm). Temperature was controlled with a temperature controller connected to the capillary furnace with a K-

DOI: 10.1021/acs.joc.5b01299
J. Org. Chem. 2015, 80, 9401−9409

type thermocouple for feedback. Owing to technical issues, the controller was set to manual mode. Because of thermal equilibration, the temperature often dropped during the course of acquisition. Only the final temperature is reported. A 0.3 mm collimator was used, and all samples were irradiated for 30 min. The peak type was analyzed by taking the reciprocal *d*-spacings and dividing them by the highest intensity peak, unless otherwise noted. Only peaks with greater than 1% intensity in the low angle region were analyzed.

Cyclic voltammetry (CV) experiments were carried out on a potentiostat that was controlled by a PC in a temperature-controlled, three-electrode cell (15 mL). The working electrode was a platinum button electrode (area = 0.020 cm^2), which was polished after each use with 0.05 m diamond slurry in an automated polisher. The reference electrode was a silver wire and the counter electrode was a Pt wire that was flame annealed prior to each use. All potentials were referenced to the ferrocene/ferricenium redox couple. Each CV experiment consisted of approximately 1−3 mM redox active species dissolved in 0.1 M tetrabutylammonium hexafluorophosphate in deoxygenated dichloromethane unless otherwise stated. All CV experiments were bubbled with Ar for 10 min prior to dissolving the redox active species, and an Ar blanket was maintained during the entire experiment. Theoretical calculations were obtained using DFT performed using Gaussian 09. The DFT calculations employed the B3LYP hybrid functional and the 6-31G+(d) basis set. All geometries were optimized in the ground state with symmetry restraints and without solvent effects. Time-dependent (TD-DFT) calculations were performed on optimized geometries. Long alkyl chains were truncated with methyl groups to simplify the calculations.

Synthesis. 1-Bromo-4-(dodecyloxy)benzene (**4a**):[48] 4-Bromophenol (2.0 g, 12 mmol), KI (1.93 g, 11.6 mmol), and K_2CO_3 (3.2 g, 23 mmol) were added to acetone (100 mL) and refluxed for 2 h. To the hot solution was added 1-bromododecane (3.0 mL, 13 mmol), and reflux was continued for 24 h. The solution was cooled and, after the acetone was removed under reduced pressure, water (100 mL) was added. The resultant mixture was extracted with methylene chloride (3 × 100 mL), and the organic portions were combined and dried with Na_2SO_4. Removal of the methylene chloride under reduced pressure followed by column chromatography using hexanes and ethyl acetate (4:1) yielded **4a** as a pure, colorless solid (3.6 g, 90%). ^{1}H NMR (300 MHz, $CDCl_3$): δ 7.36 (d, J = 9.0 Hz, 2H), 6.77 (d, J = 9.0 Hz, 2H), 3.91 (t, J = 6.6 Hz, 2H), 1.87−1.65 (m, 2H), 1.53−1.34 (m, 2H), 1.41−1.19 (m, 16H), 0.89 (t, J = 6.7 Hz, 3H). ^{13}C NMR (75 MHz, $CDCl_3$): δ 158.4, 132.3, 116.5, 112.7, 68.4, 32.1, 29.8, 29.8, 29.8, 29.7, 29.5, 29.5, 29.3, 26.2, 22.9, 14.3.

4-Dodecyloxy[(trimethylsilyl)ethynyl]benzene (**5a**):[48] Compound **4a** (250 mg, 0.732 mmol), triphenylphosphine (10 mg, 0.038 mmol), CuI (14 mg, 0.074 mmol), $Pd(PPh_3)_2Cl_2$ (26 mg, 0.037 mmol), and triethylamine (10 mL, 72 mmol) were added to a pressure flask and stirred under N_2 atmosphere. (Trimethylsilyl)acetylene (0.5 mL, 4 mmol) was added, and the mixture was heated to reflux for 16 h. After cooling, the solution was poured into water (50 mL) and extracted with methylene chloride (3 × 50 mL). The combined organic extracts were dried with Na_2SO_4, after which the methylene chloride was removed under reduced pressure. The resulting crude oil was purified using column chromatography using hexanes and ethyl acetate (4.5:0.5) to afford **5a** as a yellow oil (162 mg, 62%). ^{1}H NMR (400 MHz, $CDCl_3$): δ 7.39 (d, J = 8.9 Hz, 2H), 6.80 (d, J = 8.9 Hz, 2H), 3.94 (t, J = 6.6 Hz, 2H), 1.83−1.70 (m, 2H), 1.49−1.39 (m, 2H), 1.38−1.21 (m, 16H), 0.89 (t, J = 6.9 Hz, 3H), 0.24 (s, 9H). ^{13}C NMR (101 MHz, $CDCl_3$): δ 159.5, 133.6, 115.1, 114.5, 105.5, 92.4, 68.2, 32.1, 29.8, 29.8, 29.7, 29.7, 29.5, 29.5, 29.3, 26.2, 22.8, 14.3, 0.2.

4-Dodecyloxyethynylbenzene (**1a**):[71] Compound **5a** (75 mg, 0.21 mmol) and tetrabutylammoniumfluoride (0.5 mL of a 1.0 M solution in THF, 0.5 mmol) were combined with a mixture of THF and water (5 mL 1:1 ratio) and stirred for 16 h under N_2. The resulting reaction was extracted with $CHCl_3$ (3 × 10 mL), and the combined organic extracts were dried with Na_2SO_4. The $CHCl_3$ was removed under reduced pressure and the crude oil was purified using column chromatography using hexanes and methylene chloride (4.5:0.5) to afford **1a** as a pure yellow oil (34 mg, 57%). ^{1}H NMR (400 MHz, $CDCl_3$): δ 7.41 (d, J = 8.9 Hz, 2H), 6.83 (d, J = 8.9 Hz, 2H), 3.95 (t, J = 6.6 Hz, 2H), 2.99 (s, 1H), 1.85−1.67 (m, 2H), 1.53−1.39 (m, 1H), 1.36−1.22 (m, 16H), 0.89 (t, J = 6.9 Hz, 3H). ^{13}C NMR (101 MHz, $CDCl_3$): δ 159.7, 133.7, 114.6, 114.0, 83.9, 75.8, 68.2, 32.1, 29.8, 29.8, 29.7, 29.7, 29.5, 29.5, 29.3, 26.2, 22.8, 14.3.

2,5-Bis[(4-dodecyloxyethynylphenyl)hydroxymethyl]thiophene (**2a**): Compound **1a** (500 mg, 1.75 mmol) was added to diethyl ether (5 mL) and cooled to −78 °C. Under a N_2 atmosphere, TMEDA (0.25 mL, 1.7 mmol) and *n*BuLi (0.80 mL of a 2.1 M solution in hexanes, 1.7 mmol) were added to the initial solution and stirred for 1 h. In a separate flask, 2,5-thiophenedicarboxaldehyde (111 mg, 0.793 mmol) was added to diethyl ether (5 mL) and cooled to 0 °C in an ice bath under N_2 for 5 min before the initial hour concluded. The cooled mixture of lithiated 4-dodecyloxyethynylbenzene in diethyl ether was then transferred via cannula to the cooled solution of 2,5-thiophenedicarboxaldehyde. The resulting solution was allowed to warm to room temperature over 1 h, upon which it was quenched with water and extracted with diethyl ether (3 × 20 mL). The organic extracts were combined and dried with Na_2SO_4, after which the diethyl ether was removed under reduced pressure. The resulting crude oil was purified using column chromatography using hexanes and ethyl acetate (4:1 to 2:1) to afford **2a** as a pure yellow oil (200 mg, 35%). ^{1}H NMR (400 MHz, $CDCl_3$): δ 7.41 (d, J = 8.4 Hz, 2H), 7.11 (s, 1H), 6.83 (d, J = 8.5 Hz, 2H), 5.83 (d, J = 5.7 Hz, 1H), 3.95 (t, J = 6.5 Hz, 2H), 2.46 (s, 1H), 1.88−1.69 (m, 2H), 1.52−1.38 (m, 2H), 1.33−1.23 (m, 16H), 0.88 (t, J = 6.2 Hz, 3H). ^{13}C NMR (101 MHz, $CDCl_3$): δ 159.8, 145.8, 133.5, 125.3, 114.7, 113.9, 86.6, 86.5, 68.3, 61.2, 32.1, 29.8, 29.8, 29.7, 29.7, 29.5, 29.5, 29.3, 26.2, 22.8, 14.3. HR-MS (ESI Q-TOF): calcd for $C_{46}H_{64}SO_4Na^+$ (M + Na)$^+$, 735.4417; found, 735.4425.

5,10,15,20-Tetrakis(4-dodecyloxyethynylphenyl)-21,23-dithiaporphyrin (**3a**): Dialcohol **2a** (201 mg, 0.273 mmol) and freshly distilled pyrrole (19 μL, 0.28 mmol) were added under N_2 to methylene chloride (113 mL to achieve a concentration of 2.5 mM). The flask was wrapped in aluminum foil, subjected to $BF_3{\cdot}OEt_2$ (14 μL, 0.11 mmol), and left to stir for no longer than 5 min. DDQ (191 mg, 0.841 mmol) was then added, and the mixture was left to stir in ambient atmosphere for no longer than 5 min. The resulting mixture was then filtered through an alumina slug that had been deactivated prior (94 g of alumina, 6 mL of water, 1 mL of triethylamine) using methylene chloride as eluent. The methylene chloride was removed under reduced pressure, and the resulting crude green/black solid was subjected to column chromatography using methylene chloride and hexanes (3:1) to afford **3a** as a pure green solid (133 mg, 9%). Melting point: 128−131 °C. ^{1}H NMR (400 MHz, $CDCl_3$): δ 9.54 (s, 4H), 8.82 (s, 4H), 7.88 (d, J = 8.6 Hz, 8H), 7.02 (d, J = 8.7 Hz, 8H), 4.04 (t, J = 6.6 Hz, 8H), 1.95−1.80 (m, 8H), 1.59−1.52 (m, 8H), 1.47−1.29 (m, 64H), 0.93 (t, J = 6.8 Hz, 12H). ^{13}C NMR (101 MHz, $CDCl_3$): δ 160.1, 157.2, 148.7, 134.2, 133.8, 133.0, 115.7, 115.1, 114.6, 100.9, 89.6, 68.4, 32.1, 29.9, 29.9, 29.9, 29.7, 29.6, 29.5, 26.3, 22.9, 14.3. HR-MS (MALDI-TOF): calcd for $C_{100}H_{125}N_2S_2O_4^+$ (M + H)$^+$, 1481.9075; found, 1481.9046.

1-Bromo-4-dodecanoylbenzene:[47] Dodecanoyl chloride (20 g, 91 mmol) was added to a mixture of bromobenzene (19 mL, 0.18 mol) and aluminum chloride (18 g, 0.14 mol) and stirred for 2 h at 80 °C. After cooling, the mixture was poured into ice water and extracted with methylene chloride (3 × 100 mL). The organic extracts were combined and dried with Na_2SO_4, and the methylene chloride was removed under reduced pressure. The crude crystals were purified by recrystallization with hot ethanol to afford off-white pure crystals (7.4 g, 40%). ^{1}H NMR (400 MHz, $CDCl_3$): δ 7.82 (d, J = 8.6 Hz, 2H), 7.60 (d, J = 8.7 Hz, 2H), 2.92 (t, J = 8.8 Hz,2H), 1.75−1.68 (m, 2H), 1.40−1.20 (m, 16H), 0.88 (t, J = 6.9 Hz, 3H). ^{13}C NMR (101 MHz, $CDCl_3$): δ 199.3, 135.9, 131.9, 129.7, 128.0, 38.6, 32.0, 29.7, 29.6, 29.6, 29.4, 29.4, 24.3, 22.8, 14.2.

1-Bromo-4-dodecylbenzene (**4b**):[47] 4-Bromododecanoylbenzene (0.52 g, 1.5 mmol) was added to triethylene glycol (25 mL) and KOH (0.34 g, 6.0 mmol). Hydrazine hydrate 50−60% (0.28 mL, 4.4 mmol) was then added, and the mixture was heated at 185 °C for 16 h. The cooled solution was then poured into ice water and extracted with

DOI: 10.1021/acs.joc.5b01299
J. Org. Chem. 2015, 80, 9401−9409

methylene chloride (3 × 50 mL). The organic extracts were combined and dried with Na_2SO_4, and the methylene chloride was then removed under reduced pressure to afford a crude oil. The oil was purified using column chromatography using neat hexanes to afford **4b** as a pure yellow oil (265 mg, 58%). ^{1}H NMR (400 MHz, $CDCl_3$): δ 7.39 (d, J = 8.3 Hz, 2H), 7.05 (d, J = 8.3 Hz, 2H), 2.55 (t, J = 10 Hz, 2H), 1.62−1.54 (m, 2H), 1.34−1.24 (m, 18H), 0.89 (t, J = 6.8 Hz, 3H). ^{13}C NMR (101 MHz, $CDCl_3$): δ 142.0, 131.4, 130.3, 119.4, 29.8, 29.8, 29.7, 29.6, 29.5, 29.3.

4-Dodecyl[(trimethylsilyl)ethynyl]benzene (**5b**):[72] Compound **4b** (265 mg, 0.815 mmol), triphenylphosphine (12 mg, 0.046 mmol), CuI (17 mg, 0.089 mmol), $Pd(PPh_3)_2Cl_2$ (32 mg, 0.046 mmol), and triethylamine (15 mL, 0.11 mmol) were added to a pressure flask and stirred under N_2 atmosphere. (Trimethylsilyl)acetylene (0.6 mL, 4 mmol) was added, and the mixture was heated to reflux for 16 h. After cooling, the solution was poured into water (50 mL) and extracted with methylene chloride (3 × 50 mL). The combined organic extracts were dried with Na_2SO_4, after which the methylene chloride was removed under reduced pressure. The resulting crude oil was purified using column chromatography using hexanes and methylene chloride (4.5:0.5) to afford **5b** as a yellow oil (147 mg, 48%). ^{1}H NMR (400 MHz, $CDCl_3$): δ 7.37 (d, J = 8.2 Hz, 2H), 7.10 (d, J = 8.3 Hz, 2H), 2.58 (t, J = 11.6 Hz, 2H), 1.62−1.53 (m, 2H), 1.33−1.22 (m, 18H), 0.89 (t, J = 6.9 Hz, 3H), 0.24 (s, 9H). ^{13}C NMR (101 MHz, $CDCl_3$): δ 143.8, 132.0, 128.5, 120.4, 105.6, 93.4, 36.0, 32.1, 31.4, 29.8, 29.8, 29.7, 29.6, 29.5, 29.4, 22.8, 14.3, 0.2.

4-Dodecylethynylbenzene (**1b**):[72] Compound **5b** (147 mg, 0.429 mmol) was combined with K_2CO_3 (0.59 g, 4.3 mmol) and dissolved in a mixture (1:1) of MeOH and diethyl ether. The reaction was stirred 16 h and then washed with water and extracted with methylene chloride. All organic portions were combined and dried with Na_2SO_4, after which the solvent was removed under reduced pressure to afford a crude oil. The oil was purified with column chromatography using hexanes and ethyl acetate as eluent (4:1) to afford pure yellow oil **1b** (108 mg, 48%). ^{1}H NMR (400 MHz, $CDCl_3$): δ 7.41 (d, J = 8.2 Hz, 2H), 7.14 (d, J = 8.0 Hz, 2H), 3.03 (s, 1H), 2.61 (t, J = 11.2 Hz, 2H), 1.67−1.55 (m, 2H), 1.35−1.23 (m, 18H), 0.90 (t, J = 6.8 Hz, 3H). ^{13}C NMR (101 MHz, $CDCl_3$): δ 144.1, 132.2, 128.6, 119.4, 84.0, 76.6, 36.1, 32.1, 31.4, 29.8, 29.8, 29.7, 29.6, 29.5, 29.4, 22.98, 14.3.

2,5-Bis[(4-dodecylethynylphenyl)hydroxymethyl]thiophene (**2b**): Compound **5b** (341 mg, 1.26 mmol) was added to diethyl ether (5 mL) and cooled to −78 °C. Under a N_2 atmosphere, TMEDA (0.18 mL, 1.2 mmol) and *n*BuLi (0.57 mL of a 2.1 M solution in hexanes, 1.2 mmol) were added to the initial solution and stirred for 1 h. In a separate flask, 2,5-thiophenedicarboxaldehyde (80 mg, 0.57 mmol) was added to diethyl ether (5 mL) and cooled to 0 °C in an ice bath under N_2 for 5 min before the initial hour concluded. The cooled mixture of lithiated 4-dodecylethynylbenzene in diethyl ether was then transferred via cannula to the cooled solution of 2,5-thiophenedicarboxaldehyde. The resulting solution was allowed to warm to room temperature over 1 h, upon which it was quenched with water and extracted with diethyl ether (3 × 20 mL). The organic extracts were combined and dried with Na_2SO_4, after which the diethyl ether was removed under reduced pressure. The resulting crude oil was purified using column chromatography using a hexanes and ethyl acetate (4:1 to 2:1) to afford **2b** as a pure yellow oil (200 mg, 52%). ^{1}H NMR (400 MHz, $CDCl_3$): δ 7.40 (d, J = 8.1 Hz, 2H), 7.13 (d, J = 8.0 Hz, 2H), 7.10 (s, 1H), 5.83 (s, 1H), 2.88 (s, 1H), 2.60 (t, J = 11.2 Hz, 2H), 1.65−1.55 (m, 2H), 1.38−1.22 (m, 18H), 0.90 (t, J = 6.8 Hz, 3H). ^{13}C NMR (101 MHz, $CDCl_3$): δ 145.6, 144.1, 131.9, 128.5, 125.3, 119.3, 87.3, 86.6, 61.0, 36.0, 32.0, 31.3, 29.8, 29.8, 29.8, 29.7, 29.6, 29.5, 29.4, 22.8, 14.2. HR-MS (ESI Q-TOF): calcd for $C_{46}H_{64}SO_2Na^+$ $(M + Na)^+$, 703.4519; found, 703.4532.

5,10,15,20-Tetrakis(4-dodecylethynylphenyl)-21,23-dithiaporphyrin (**3b**): Dialcohol **2b** (111 mg, 0.158 mmol) and freshly distilled pyrrole (11 μL, 0.16 mmol) were added under N_2 to methylene chloride (64 mL to achieve a concentration of 2.5 mM). The flask was wrapped in aluminum foil, subjected to $BF_3{\cdot}OEt_2$ (8 μL, 0.06 mmol), and left to stir for no longer than 5 min. DDQ (109 mg, 0.480 mmol) was then added, and the mixture was left to stir in ambient atmosphere for no longer than 5 min. The resulting mixture was then filtered through an alumina slug that had been previously deactivated (94 g of alumina, 6 mL of water, 1 mL of triethylamine) using methylene chloride as eluent. The methylene chloride was removed under reduced pressure, and the resulting crude green/black solid was subjected to column chromatography using methylene chloride and hexanes (3:1) to afford **3b** as a pure green solid (16 mg, 7%). Melting point: 108−118 °C. ^{1}H NMR (400 MHz, $CDCl_3$): δ 9.67 (s, 4H), 8.92 (s, 4H), 7.94 (d, J = 8.0 Hz, 8H), 7.39 (d, J = 8.0 Hz, 8H), 2.83−2.75 (m, 8H), 1.79 (m, 8H), 1.53−1.44 (m, 8H), 1.44−1.29 (m, 64H), 0.92 (t, J = 6.8 Hz, 12H). ^{13}C NMR (101 MHz, $CDCl_3$): δ 157.3, 148.9, 144.5, 134.2, 133.1, 132.2, 129.0, 121.0, 114.2, 100.8, 90.1, 36.4, 32.1, 31.6, 29.9, 29.9, 29.9, 29.9, 29.8, 29.7, 29.6, 22.9, 14.3. HR-MS (MALDI-TOF): calcd for $C_{100}H_{125}N_2S_2$ $(M + H)^+$, 1417.9279; found, 1417.9228.

2,5-thiophenedicarboxaldehyde:[73] Thiophene (1.0 mL, 13 mmol) was added to a solution of 2.2 M *n*BuLi (12.2 mL, 27.5 mmol) and TMEDA (4.0 mL, 28 mmol) in 100 mL of hexanes. The solution was refluxed for 1 h and then cannula transferred into a solution of DMF (2.1 mL, 28 mmol) in 50 mL of hexanes at 0 °C and stirred an additional hour. The reaction was quenched with 1.0 M HCl and extracted with ether (3 × 50 mL). The organic layer was dried with Na_2SO_4, and then the solvent was removed under reduced pressure. The crude solid was purified using column chromatography using hexanes and ethyl acetate (4:1) to afford the title compound as a bright yellow solid (1.33 g, 76%).^{1}H NMR (400 MHz, $CDCl_3$): δ 10.02 (s, 1H), 7.84 (s, 1H). ^{13}C NMR (101 MHz, $CDCl_3$): δ 183.6, 149.3, 135.2.

■ ASSOCIATED CONTENT

Supporting Information

The Supporting Information is available free of charge on the ACS Publications website at DOI: 10.1021/acs.joc.5b01299.

^{1}H and ^{13}C NMR as well as additional optical, electrochemical, XRD and DFT data (PDF)

■ AUTHOR INFORMATION

Corresponding Author

*E-mail: todd.sutherland@ucalgary.ca.

Notes

The authors declare no competing financial interest.

■ ACKNOWLEDGMENTS

T.C.S. thanks NSERC of Canada (RGPIN/04444-2014) for financial support and WestGrid/Compute Canada for use of their computing resources to carry out DFT research. A.D.B. thanks Alberta Innovates Technology Futures for a scholarship. S.N.K. thanks NSERC of Canada and Alberta Innovates Technology Futures for scholarship support. V.E.W. thanks NSERC of Canada (RGPIN/238724-2011) for financial assistance.

■ REFERENCES

(1) Kadish, K. M.; Smith, K. M.; Guilard, R. *The Porphyrin Handbook: Applications: past, present, and future*; Academic Press: San Diego, CA, 1999; Vol. 6.

(2) Mazière, J. C.; Morlière, P.; Santus, R. *J. Photochem. Photobiol., B* **1991**, *8* (4), 351−360.

(3) Lovell, J. F.; Chan, M. W.; Qi, Q.; Chen, J.; Zheng, G. *J. Am. Chem. Soc.* **2011**, *133* (46), 18580−18582.

(4) Yella, A.; Lee, H.-W.; Tsao, H. N.; Yi, C.; Chandiran, A. K.; Nazeeruddin, M. K.; Diau, E. W.-G.; Yeh, C.-Y.; Zakeeruddin, S. M.; Grätzel, M. *Science* **2011**, *334* (6056), 629−634.

(5) Griffith, M. J.; Sunahara, K.; Wagner, P.; Wagner, K.; Wallace, G. G.; Officer, D. L.; Furube, A.; Katoh, R.; Mori, S.; Mozer, A. J. *Chem. Commun.* **2012**, *48* (35), 4145−4162.

DOI: 10.1021/acs.joc.5b01299
J. Org. Chem. 2015, 80, 9401−9409

(6) Qin, H.; Li, L.; Guo, F.; Su, S.; Peng, J.; Cao, Y.; Peng, X. *Energy Environ. Sci.* **2014**, *7* (4), 1397−1401.
(7) Sun, Q.; Dai, L.; Zhou, X.; Li, L.; Li, Q. *Appl. Phys. Lett.* **2007**, *91* (25), 253505.
(8) Walter, M. G.; Rudine, A. B.; Wamser, C. C. *J. Porphyrins Phthalocyanines* **2010**, *14* (09), 759−792.
(9) Kadish, K. M.; Smith, K. M.; Guilard, R. *The Porphyrin Handbook: Synthesis and Organic Chemistry*; Academic Press: San Diego, CA, 2000; Vol. *1*.
(10) Lindsey, J. S.; Hsu, H. C.; Schreiman, I. C. *Tetrahedron Lett.* **1986**, *27* (41), 4969−4970.
(11) Adler, A. D.; Longo, F. R.; Finarelli, J. D.; Goldmacher, J.; Assour, J.; Korsakoff, L. *J. Org. Chem.* **1967**, *32* (2), 476−476.
(12) You, Y.; Gibson, S. L.; Hilf, R.; Davies, S. R.; Oseroff, A. R.; Roy, I.; Ohulchanskyy, T. Y.; Bergey, E. J.; Detty, M. R. *J. Med. Chem.* **2003**, *46* (17), 3734−3747.
(13) Punidha, S.; Ravikanth, M. *Tetrahedron* **2004**, *60* (38), 8437−8444.
(14) Punidha, S.; Agarwal, N.; Ravikanth, M. *Eur. J. Org. Chem.* **2005**, *2005* (12), 2500−2517.
(15) Punidha, S.; Agarwal, N.; Burai, R.; Ravikanth, M. *Eur. J. Org. Chem.* **2004**, *2004* (10), 2223−2230.
(16) Bromby, A. D.; Kan, W. H.; Sutherland, T. C. *J. Mater. Chem.* **2012**, *22* (38), 20611−20617.
(17) Bromby, A. D.; Jansonius, R. P.; Sutherland, T. C. *J. Org. Chem.* **2013**, *78* (4), 1612−1620.
(18) Plater, M. J.; Aiken, S.; Bourhill, G. *Tetrahedron* **2002**, *58* (12), 2405−2413.
(19) Kuo, M.-C.; Li, L.-A.; Yen, W.-N.; Lo, S.-S.; Lee, C.-W.; Yeh, C.-Y. *Dalton Trans.* **2007**, No. 14, 1433−1439.
(20) Ragoussi, M.-E.; de la Torre, G.; Torres, T. *Eur. J. Org. Chem.* **2013**, *2013* (14), 2832−2840.
(21) Gradillas, A.; del Campo, C.; Sinisterra, J. V.; Llama, E. F. *J. Chem. Soc., Perkin Trans. 1* **1995**, No. 20, 2611−2613.
(22) Geier, G. R.; Riggs, J. A.; Lindsey, J. S. *J. Porphyrins Phthalocyanines* **2001**, *05* (09), 681−690.
(23) Arnold, D. P.; Johnson, A. W.; Mahendran, M. *J. Chem. Soc., Perkin Trans. 1* **1978**, No. 4, 366−70.
(24) Anderson, H. L. *Tetrahedron Lett.* **1992**, *33* (8), 1101−1104.
(25) Lin, V. S. Y.; DiMagno, S. G.; Therien, M. J. *Science (Washington, DC, U. S.)* **1994**, *264* (5162), 1105−11.
(26) Boyle, R. W.; Johnson, C. K.; Dolphin, D. *J. Chem. Soc., Chem. Commun.* **1995**, No. 5, 527−8.
(27) Yella, A.; Lee, H.-W.; Tsao, H. N.; Yi, C.; Chandiran, A. K.; Nazeeruddin, M. K.; Diau, E. W.-G.; Yeh, C.-Y.; Zakeeruddin, S. M.; Graetzel, M. *Science (Washington, DC, U. S.)* **2011**, *334* (6056), 629−634.
(28) Mathew, S.; Yella, A.; Gao, P.; Humphry-Baker, R.; Curchod, B. F. E.; Ashari-Astani, N.; Tavernelli, I.; Rothlisberger, U.; Nazeeruddin, M. K.; Graetzel, M. *Nat. Chem.* **2014**, *6* (3), 242−247.
(29) Kubo, Y.; Yamamoto, M.; Ikeda, M.; Takeuchi, M.; Shinkai, S.; Yamaguchi, S.; Tamao, K. *Angew. Chem., Int. Ed.* **2003**, *42* (18), 2036−2040.
(30) Screen, T. E. O.; Thorne, J. R. G.; Denning, R. G.; Bucknall, D. G.; Anderson, H. L. *J. Am. Chem. Soc.* **2002**, *124* (33), 9712−9713.
(31) Ogawa, K.; Ohashi, A.; Kobuke, Y.; Kamada, K.; Ohta, K. *J. Am. Chem. Soc.* **2003**, *125* (44), 13356−13357.
(32) Drobizhev, M.; Stepanenko, Y.; Dzenis, Y.; Karotki, A.; Rebane, A.; Taylor, P. N.; Anderson, H. L. *J. Am. Chem. Soc.* **2004**, *126* (47), 15352−15353.
(33) Anderson, H. L. *Inorg. Chem.* **1994**, *33* (5), 972−81.
(34) Taylor, P. N.; Anderson, H. L. *J. Am. Chem. Soc.* **1999**, *121* (49), 11538−11545.
(35) Ghoroghchian, P. P.; Frail, P. R.; Susumu, K.; Blessington, D.; Brannan, A. K.; Bates, F. S.; Chance, B.; Hammer, D. A.; Therien, M. J. *Proc. Natl. Acad. Sci. U. S. A.* **2005**, *102* (8), 2922−2927.
(36) Milgrom, L. R.; Yahioglu, G. *Tetrahedron Lett.* **1996**, *37* (23), 4069−4072.
(37) Milgrom, L. R.; Yahioglu, G. *Tetrahedron Lett.* **1995**, *36* (49), 9061−9064.
(38) McEwan, K. J.; Bourhill, G.; Robertson, J. M.; Anderson, H. L. *J. Nonlinear Opt. Phys. Mater.* **2000**, *9* (4), 451.
(39) Anderson, H.; Wylie, A.; Prout, K. *J. Chem. Soc., Perkin Trans. 1* **1998**, No. 10, 1607−1612.
(40) Milgrom, L. R.; Rees, R. D.; Yahioglu, G. *Tetrahedron Lett.* **1997**, *38* (27), 4905−4908.
(41) Nowak-Król, A.; Łukasiewicz, Ł. G.; Haley, J. E.; Drobizhev, M.; Rebane, A.; Cooper, T. M.; Gryko, D. T. *J. Porphyrins Phthalocyanines* **2014**, *18* (10n11), 998−1013.
(42) Berlicka, A.; Latos-Grażyński, L.; Lis, T. *Inorg. Chem.* **2005**, *44* (13), 4522−4533.
(43) Samarat, A.; Kuninobu, Y.; Takai, K. *Synlett* **2011**, *2011* (15), 2177−2180.
(44) Spence, J. D.; Lash, T. D. *J. Org. Chem.* **2000**, *65* (5), 1530−1539.
(45) Shen, Z.; Uno, H.; Shimizu, Y.; Ono, N. *Org. Biomol. Chem.* **2004**, *2* (23), 3442−3447.
(46) Ulman, A.; Manassen, J. *J. Am. Chem. Soc.* **1975**, *97* (22), 6540−6544.
(47) Wehmeier, M.; Wagner, M.; Müllen, K. *Chem. - Eur. J.* **2001**, *7* (10), 2197−2205.
(48) Weiss, K.; Beernink, G.; Dötz, F.; Birkner, A.; Müllen, K.; Wöll, C. H. *Angew. Chem., Int. Ed.* **1999**, *38* (24), 3748−3752.
(49) Rao, P. D.; Dhanalekshmi, S.; Littler, B. J.; Lindsey, J. S. *J. Org. Chem.* **2000**, *65* (22), 7323−7344.
(50) Cho, W.-S.; Kim, H.-J.; Littler, B. J.; Miller, M. A.; Lee, C.-H.; Lindsey, J. S. *J. Org. Chem.* **1999**, *64* (21), 7890−7901.
(51) Barnett, G. H.; Hudson, M. F.; Smith, K. M. *J. Chem. Soc., Perkin Trans. 1* **1975**, No. 14, 1401−1403.
(52) Anderson, H. L.; Wylie, A. P.; Prout, K. *J. Chem. Soc., Perkin Trans. 1* **1998**, No. 10, 1607−1612.
(53) Liu, Z.-B.; Zhu, Y.; Zhu, Y.-Z.; Tian, J.-G.; Zheng, J.-Y. *J. Phys. Chem. B* **2007**, *111* (51), 14136−14142.
(54) Thompson, B. C.; Fréchet, J. M. J. *Angew. Chem., Int. Ed.* **2008**, *47* (1), 58−77.
(55) Winder, C.; Matt, G.; Hummelen, J. C.; Janssen, R. A. J.; Sariciftci, N. S.; Brabec, C. J. *Thin Solid Films* **2002**, *403*−*404* (0), 373−379.
(56) Brabec, C. J.; Winder, C.; Sariciftci, N. S.; Hummelen, J. C.; Dhanabalan, A.; van Hal, P. A.; Janssen, R. A. J. *Adv. Funct. Mater.* **2002**, *12* (10), 709−712.
(57) Ulman, A.; Manassen, J.; Frolow, F.; Rabinovich, D. *Inorg. Chem.* **1981**, *20* (7), 1987−1990.
(58) Kadish, K. M.; Morrison, M. M. *J. Am. Chem. Soc.* **1976**, *98* (11), 3326−3328.
(59) Scharber, M. C.; Mühlbacher, D.; Koppe, M.; Denk, P.; Waldauf, C.; Heeger, A. J.; Brabec, C. J. *Adv. Mater.* **2006**, *18* (6), 789−794.
(60) Gomer, R.; Tryson, G. *J. Chem. Phys.* **1977**, *66* (10), 4413−4424.
(61) Frisch, M. J.; Trucks, G. W.; Schlegel, H. B.; Scuseria, G. E.; Robb, M. A.; Cheeseman, J. R.; Scalmani, G.; Barone, V.; Mennucci, B.; Petersson, G. A.; Nakatsuji, H.; Caricato, M.; Li, X.; Hratchian, H. P.; Izmaylov, A. F.; Bloino, J.; Zheng, G.; Sonnenberg, J. L.; Hada, M.; Ehara, M.; Toyota, K.; Fukuda, R.; Hasegawa, J.; Ishida, M.; Nakajima, T.; Honda, Y.; Kitao, O.; Nakai, H.; Vreven, T.; Montgomery, J. A., Jr.; Peralta, J. E.; Ogliaro, F.; Bearpark, M. J.; Heyd, J.; Brothers, E. N.; Kudin, K. N.; Staroverov, V. N.; Kobayashi, R.; Normand, J.; Raghavachari, K.; Rendell, A. P.; Burant, J. C.; Iyengar, S. S.; Tomasi, J.; Cossi, M.; Rega, N.; Millam, N. J.; Klene, M.; Knox, J. E.; Cross, J. B.; Bakken, V.; Adamo, C.; Jaramillo, J.; Gomperts, R.; Stratmann, R. E.; Yazyev, O.; Austin, A. J.; Cammi, R.; Pomelli, C.; Ochterski, J. W.; Martin, R. L.; Morokuma, K.; Zakrzewski, V. G.; Voth, G. A.; Salvador, P.; Dannenberg, J. J.; Dapprich, S.; Daniels, A. D.; Farkas, Ö.; Foresman, J. B.; Ortiz, J. V.; Cioslowski, J.; Fox, D. J. *Gaussian 09*; Gaussian, Inc.: Wallingford, CT, 2009.
(62) Nguyen, K. A.; Pachter, R. *J. Chem. Phys.* **2001**, *114* (24), 10757.

DOI: 10.1021/acs.joc.5b01299
J. Org. Chem. 2015, 80, 9401−9409

(63) Zandler, M. E.; D'Souza, F. *C. R. Chim.* **2006**, *9* (7−8), 960−981.
(64) Liao, M.-S.; Watts, J. D.; Huang, M.-J. *J. Comput. Chem.* **2006**, *27* (13), 1577−1592.
(65) Wang, Z.; Day, P. N. *J. Chem. Phys.* **1998**, *108* (6), 2504.
(66) Acree, W. E.; Chickos, J. S. *J. Phys. Chem. Ref. Data* **2006**, *35* (3), 1051.
(67) Mudring, A.-V.; Stappert, K.; Unal, D.; Mallick, B. *J. Mater. Chem. C* **2014**, *2*, 7976.
(68) Kadish, K. M.; Smith, K. M.; Guilard, R. *The Porphyrin Handbook: Applications: past, present, and future*; Academic Press: San Diego, CA, 1999.
(69) Li, L.; Kang, S. W.; Harden, J.; Sun, Q.; Zhou, X.; Dai, L.; Jakli, A.; Kumar, S.; Li, Q. *Liq. Cryst.* **2008**, *35* (3), 233−239.
(70) Lavigueur, C.; Foster, E. J.; Williams, V. E. *J. Appl. Crystallogr.* **2008**, *41* (1), 214−216.
(71) Kitamura, T.; Lee, C. H.; Taniguchi, H.; Matsumoto, M.; Sano, Y. *J. Org. Chem.* **1994**, *59* (26), 8053−8057.
(72) Tlach, B. C.; Tomlinson, A. L.; Bhuwalka, A.; Jeffries-El, M. *J. Org. Chem.* **2011**, *76* (21), 8670−8681.
(73) De, P. K.; Neckers, D. C. *Org. Lett.* **2012**, *14* (1), 78−81.

DOI: 10.1021/acs.joc.5b01299
J. Org. Chem. 2015, 80, 9401−9409